

Article

Solution Properties of Water-Soluble “Smart” Poly(*N*-acryloyl-*N'*-ethyl piperazine-*co*-methyl methacrylate)

G. Roshan Deen

Soft Materials Laboratory, Natural Sciences and Science Education, National Institute of Education, Nanyang Technological University, 1-Nanyang Walk, 637616, Singapore;
E-Mail: Roshan.gulam@nie.edu.sg; Tel.: +65-6790-3826; Fax: +65-6896-9414

Received: 28 November 2011; in revised form: 21 December 2011 / Accepted: 5 January 2012 /
Published: 5 January 2012

Abstract: Water-soluble copolymers of *N*-acryloyl-*N'*-ethylpiperazine (AcrNEP) with methyl methacrylate (MMA) were synthesized to high conversion by free-radical solution polymerization. The composition of the copolymers was determined using Fourier Transform Infra-red Spectroscopy (FTIR). Copolymers containing AcrNEP content above 44 mol% were readily soluble in water and exhibited the critical solution temperature behavior. The copolymers were strongly responsive to changes in pH of the external medium due to the presence of tertiary amine functions that could be protonated at low pH. The influence of various factors such as copolymer composition, pH, temperature, salt and surfactant concentration on the LCST of the copolymers were systematically studied. The intrinsic viscosity of the copolymers in dimethyl formamide decreased with increase in temperature due to a decrease in thermodynamic affinity between polymer chains and solvent molecules. The viscosity behavior of the copolymers in sodium chloride solution was similar to that of classical polyelectrolytes and hydrophobically modified polyacrylate systems.

Keywords: water-soluble polymers; piperazine; viscosity; critical solution temperature

1. Introduction

Water-soluble polymers that respond to external stimuli such as pH, temperature, electrolytes, illumination, electric and magnetic field are called as smart, stimuli-responsive, intelligent, or environmentally sensitive polymers [1–3]. Recent interest in intelligent polymeric systems has focused on aqueous solutions, interfaces, nanogels, and hydrogels due to their promising applications in

targeted drug delivery systems, immobilization of enzymes, cell encapsulation, ordered porous materials, chemical sensors *etc.* [2–5]. These polymers are soluble in water at low temperatures but separate from solution when the temperature is raised above a certain temperature called the lower critical solution temperature (LCST). Poly(*N*-isopropyl acrylamide) (PNIPAM) is one of the most widely studied thermo-responsive polymer, which undergoes phase separation in water around 32 °C [6–10]. This polymer has both hydrophilic and hydrophobic groups. At lower temperatures water is a good solvent and forms hydrogen bonds with the hydrophilic groups. With increase in temperature the hydrogen bonds are broken and hydrophobic interaction between the polymer chains become dominant leading to a phase separation of the polymer from the solution.

A critical balance of hydrophilic and hydrophobic side groups of the polymer system is a vital parameter for observing the LCST behavior. The introduction of hydrophilic and hydrophobic co-monomers can cause the LCST to either increase or decrease. The nature of chemical moieties of the polymer also plays a vital role in influencing the LCST. The addition of one or two methylene groups to the monomer unit can convert the polymer from being totally soluble in water to one with LCST behavior. This is due to an entropy phenomenon, and the entropy change for the transfer of a methylene group into water has been reported to be $-20 \text{ J}^{-1} \cdot \text{deg}^{-1} \cdot \text{mol}$.

In recent years, polymer systems that respond to more than one stimulus such as pH and temperature have received considerable research attention [11–14]. To prepare polymers that respond to more than one stimulus, monomers that are sensitive to certain stimuli have to be copolymerized. In this paper, the synthesis of a ‘stimuli’-responsive piperazine-containing new copolymers is reported. These copolymers are water soluble and exhibit interesting LCST behavior. The phase transition of the copolymers is sensitive to a number of factors such as monomer composition, pH, temperature, salts, and surfactants. The influence of these factors is described in detail in this report.

2. Experimental Section

2.1. Materials

Acryloyl chloride (Aldrich) and methyl methacrylate (MMA) (Aldrich) were distilled under reduced pressure and stored in the refrigerator. *N*-ethyl piperazine (Aldrich) was stored over dry molecular sieves of pore size 3 Å prior to use. Azobisisobutyronitrile (AIBN) (TCI) was recrystallized in methanol. 1,4-dioxane (Merck) and tetrahydrofuran (Aldrich) were refluxed with metallic sodium for 3 h and distilled under nitrogen. Deionized water from an ion exchange system (Barnstead D4755, USA) was used for all aqueous sample preparations.

2.2. Synthesis of *N*-Acryloyl-*N'*-ethyl piperazine (AcrNEP)

The monomer AcrNEP was synthesized by the method described previously [15]. *N*-ethyl piperazine (0.18 mol, 20.0 g), triethylamine (0.18 mol, 18.2 g) were dissolved in dry THF (400 mL) in a 1 litre three-neck Claisen flask fitted with a nitrogen inlet and a guard tube. The flask was cooled in an ice-bath and the reaction mixture was maintained in an inert atmosphere by purging with dry nitrogen gas. Acryloyl chloride (0.18 mol, 15.9 g) dissolved in dry THF (50 mL) was added in drops for a period of 30 min using a pressure equalizing funnel. The reaction mixture was stirred vigorously

and allowed to equilibrate to room temperature after the complete addition of acryloyl chloride. Triethylamine hydrochloride was removed by filtration and the filtrate was concentrated to a brown viscous liquid. The brown viscous liquid was distilled under reduced pressure to obtain the monomer as pale yellow oil (Yield: 80%; n_D^{20} : 1.5060).

2.3. Synthesis of Copolymers

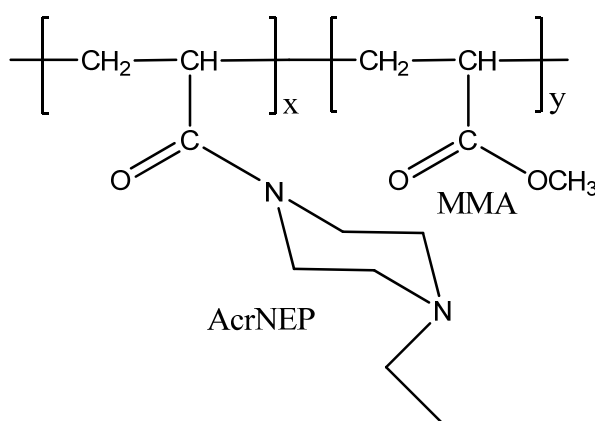
Statistical linear copolymers of AcrNEP and MMA with various monomer feed ratios were prepared by free-radical solution polymerization. Typically, AcrNEP (0.7 mmol), MMA (9.3 mmol), and AIBN (0.5 wt%) were dissolved in freshly distilled 1,4-dioxane (25 mL) in a round bottom flask fitted with a glass tap. The content was degassed three times by freeze-thaw cycle and the flask was sealed under vacuum. Polymerization was carried out at 75 °C for 24 h. The flask was air cooled to room temperature and the content was poured into diethyl ether (400 mL) to isolate the copolymer. The copolymer was purified by free drying using water as solvent. Similar linear copolymers were prepared using various monomer feed ratios and the data are summarized in Table 1. The structure of the copolymer is shown in Figure 1.

Table 1. Feed compositions in the synthesis and characterization of copolymers.

Copolymer	X^{Feed}		$X^{\text{Copolymer}}$		$M_w \times 10^{-5}$ ($\text{g}\cdot\text{mol}^{-1}$)	pK_{ap}
	AcrNEP	MMA	AcrNEP	MMA		
BCP-1	0.5200	0.4799	0.4412	0.5588	0.95	4.65
BCP-2	0.6236	0.3764	0.5502	0.4498	0.91	4.66
BCP-3	0.6982	0.3018	0.6017	0.3983	0.89	4.66
BCP-4	0.7618	0.2382	0.6627	0.3374	0.97	4.66

X = mole fraction.

Figure 1. Chemical structure of the copolymer.



2.4. Characterization

The composition of the copolymers was determined by infra-red spectral analysis on Perkin-Elmer (Spectrum 100) FTIR spectrophotometer. The copolymers were analyzed as thin films on sodium chloride windows by the method described previously [15].

The solubility of the copolymers was studied in various solvents. About 2 mL of each solvent was added to about 0.02 g of the polymer in a screw capped glass vial. The mixture was allowed to stand for 24 h at 23 °C, and a visual observation on the solubility was recorded.

The weight-average molecular weight (M_w), the second-virial co-efficient (A_2), and the hydrodynamic radius (R_h) of the copolymers was determined using a Zetasizer (Malvern Zetasizer ZS90) with a Helium-Neon laser ($\lambda = 633$ nm). The copolymer samples in distilled THF were filtered three times through a syringe filter (Teflon, 0.45 micron) into a clean rectangular quartz cell. For the determination of M_w , the scattered light intensity of six different concentration of the polymer sample was measured at a scattering angle of 90°. The M_w and A_2 were determined by the Debye approximation as,

$$\frac{Kc}{R(\theta)} = \frac{1}{M_w} + 2A_2 c \quad (1)$$

where K , $R(\theta)$, and c are the optical constant, Rayleigh ratio, and polymer concentration respectively. The optical constant K is defined as,

$$K = \frac{4\pi^2 n_o^2}{\lambda^4 N_A} \left(\frac{dn}{dc} \right)^2 \quad (2)$$

where n_o , λ , N_A , and dn/dc are the refractive index of toluene, wavelength of laser, Avogadro's constant, and the refractive index increment of the polymer respectively.

For the determination of R_h , the normalized intensity-time auto-correlation function ($g_2(t) - 1$) was measured for 60 s. The auto-correlations were analyzed by Laplace inversion using the model-independent CONTIN program to obtain the average R_h by the Stokes-Einstein relation as,

$$R_h = \frac{k_B T}{6\pi\eta D} \quad (3)$$

where k_B , T , η , and D are the Boltzmann constant, temperature, viscosity of the solvent, and diffusion respectively.

The LCST of the copolymers were determined both by visual observation and on a UV/Vis spectrophotometer attached with a temperature control. Polymer solutions of 1 wt% were used in this study.

Differential scanning calorimetric measurements were recorded using a Perkin-Elmer diamond DSC. About 10 mg of polymer sample sealed in aluminum pan was used for this measurement. All measurements were carried out under a stream of dry nitrogen with a heating rate of 20 °C·min⁻¹. The glass transition temperature (T_g) was determined from the mid-point of the inflection of the thermogram.

Micro calorimetric measurements were recorded on a Microcal MC-2 high sensitivity differential scanning calorimeter (Microcal, Northampton, USA). Both the polymer solution and water (reference) were degassed and transferred to the cells using long needle syringes (Hamilton). The enthalpy change for the transition (ΔH) was calculated from the area of the transition peak, and LCST was determined from the maximum of the first derivative of the heat capacity *versus* temperature plot.

Potentiometric titrations of the polymers were performed using an ABU93 Triburette Titration System (Radiometer, Denmark). The instrument was integrated with a standard RS232C interface and the titration was controlled using the ALIQUOT titration software. The electrode assembly consisted of an Orion pHg201 glass electrode and an Orion REF201 reference electrode. The conductivity was measured using a CDM83 conductivity meter.

3. Results and Discussion

3.1. Synthesis of Copolymers and Solubility

The copolymers were synthesized by free-radical polymerization in solution (dioxane) using AIBN as the thermal free-radical initiator. The copolymers were obtained as white powder. With increase in AcrNEP content the copolymers were hygroscopic. All the copolymers prepared were soluble in water, methanol, chloroform, and THF at room temperature (23 °C). The solubility is dependent on the AcrNEP content in the copolymer and when the amount is greater than 44 mol%, water solubility is achieved. Hence a proper balance of hydrophilic and hydrophobic groups is necessary in developing water-soluble polymers for desired applications.

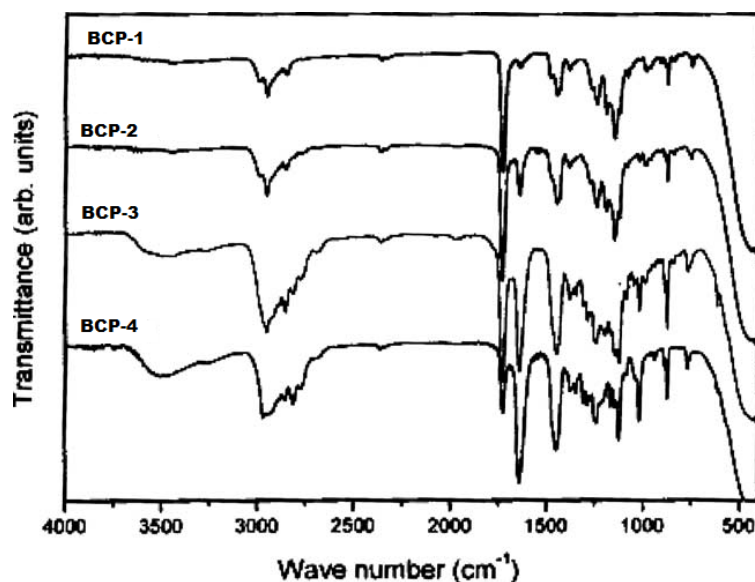
3.2. FTIR Spectroscopy and Copolymer Composition

The FTIR spectra of the copolymers (as thin films on NaCl plates) are shown in Figure 2. The main characteristic feature is the absence of the vinyl double bond absorption peak at around 1,600 cm^{-1} . This indicates the conversion of the vinyl double bond of the monomers AcrNEP and MMA. The intense peaks (cm^{-1}) at around 1,728 and 1,636 are the absorption peaks of the carbonyl group of MMA (ester) and AcrNEP (amide) respectively. At high AcrNEP content, the copolymer was hygroscopic as mentioned earlier and this is reflected as a broad absorption peak at 3,400 cm^{-1} (water). The composition of the copolymers was calculated based on the following equation,

$$\left[\frac{\text{MMA}}{\text{AcrNEP}} \right] = \frac{A_{\text{MMA}}}{A_{\text{AcrNEP}}} \times \frac{\epsilon_{\text{AcrNEP}}}{\epsilon_{\text{MMA}}} \quad (4)$$

where A_{MMA} , ϵ_{MMA} , A_{AcrNEP} , and ϵ_{AcrNEP} are the absorbance and molar extinction coefficient of MMA ($300 \text{ dm}^3 \cdot \text{mol}^{-1} \cdot \text{cm}^{-1}$) of MMA, and absorbance and molar extinction coefficient of AcrNEP ($330 \text{ dm}^3 \cdot \text{mol}^{-1} \cdot \text{cm}^{-1}$) respectively. The copolymer compositions are given in Table 1 along with monomer feed ratios.

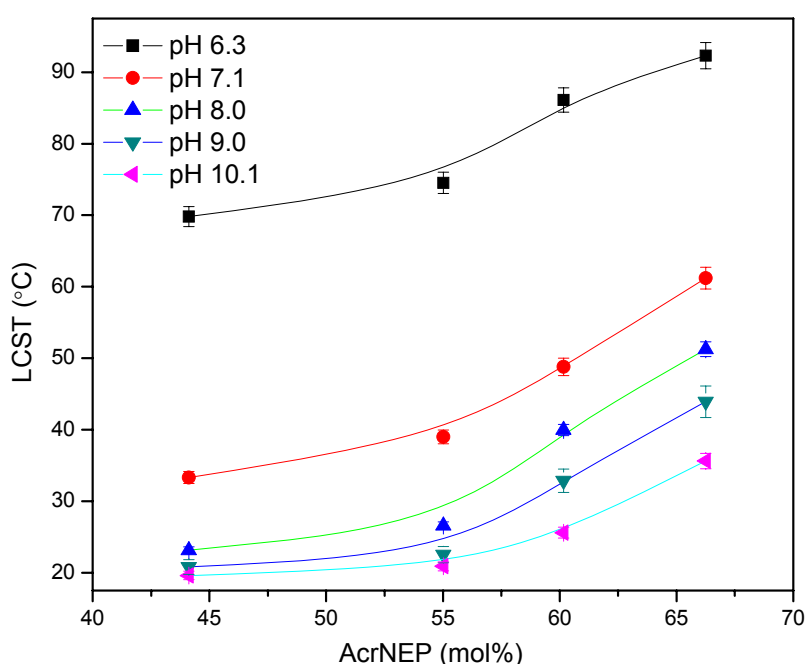
Figure 2. FTIR spectra of copolymers obtained as thin films on NaCl window.



3.3. Lower Critical Solution Temperature (LCST) in Water and Buffer Solution

The critical solution temperature is defined as the temperature at which a polymer in aqueous solution undergoes a reversible macromolecular phase transition from a hydrophilic to a hydrophobic structure. Such transitions are also termed as the coil-to-globule type transitions. The homopolymer of AcrNEP did not exhibit any LCST while the copolymers containing 44 mol% of AcrNEP showed LCST phenomenon. The LCST of the copolymers was studied in water and buffer solutions (pH 6, 7, 8, 10). The LCST values obtained from the maxima of first derivatives of the transmittance (%) versus temperature curves are shown in Figure 3. The results clearly show that the copolymers are highly sensitive to pH.

Figure 3. Effect of copolymer composition and solution pH on the LCST.



The LCST is higher in acidic solution (pH 6.3) and lower in basic solutions (pH 8–10). For a very small change of 0.8 on pH scale from pH 6.3 to 7.1, a difference of 35 °C in LCST is observed for the copolymer BCP-1. The pH effect in tuning the LCST is attributed to the various degree of protonation on the basic tertiary amino group of AcrNEP unit. It should be noted that AcrNEP is a poly amido-amine which contains an amide and a tertiary amine group. Protonation gives rise to electrostatic repulsion between the fixed charges on the macromolecule which results in higher phase transition temperatures in solutions of low pH. In basic solutions, the protonation is weak and polymer-polymer interaction (hydrophobic interaction) is achieved at lower temperatures. The effect of AcrNEP content on the LCST is also observed in Figure 3. At a fixed pH, the LCST increases with increasing AcrNEP monomer content in the copolymer. This again is a consequence of protonation and charge repulsion behaviour between the AcrNEP monomer units. In addition to the critical balance between the hydrophilic-hydrophobic groups in the copolymer, the pK_a of the tertiary amine and the charge density could also affect the LCST of these polymers.

In order to study the effect of charge on the phase separation potentiometric titration of the copolymers were performed using 0.12 M HCl (without added electrolyte). From the titration curves, the apparent dissociation constant (pK_{ap}) of the copolymers was calculated using the following expression,

$$pK_{ap} = pH - \frac{\log \alpha}{(1 - \alpha)} \quad (5)$$

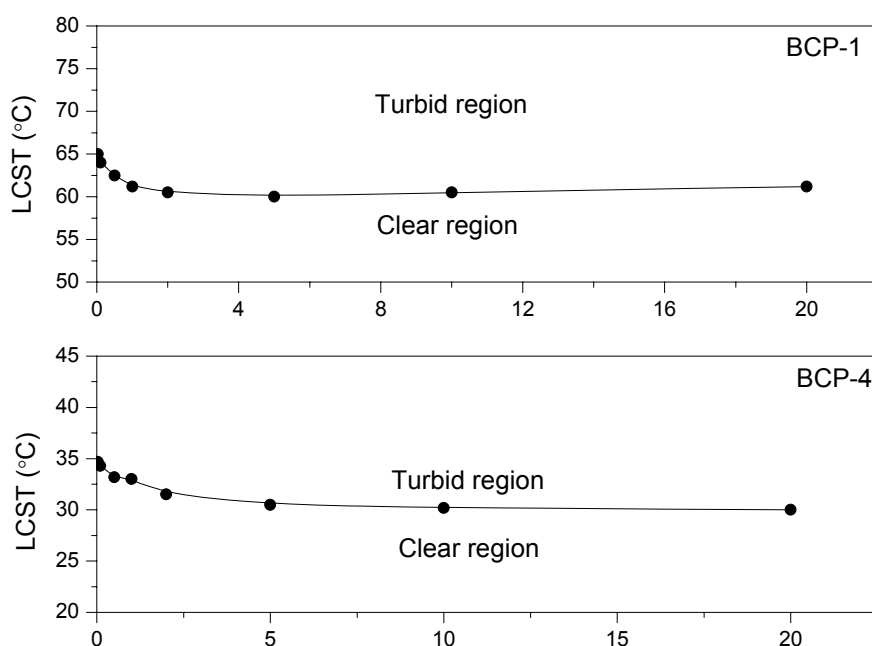
where α is the degree of protonation. This is defined as,

$$\alpha = \frac{C_H}{C_m} \quad (6)$$

where C_H is the effective concentration of added HCl and C_m is the concentration of the polymer chains in terms of monomer units. This equation implies that all of H^+ added from HCl is assumed to protonate the amine groups. The pK_{ap} of the copolymers determined are summarized in Table 1. The apparent dissociation constant shows a slight increase with increase in AcrNEP content in the copolymer. Using these values the total amount of charged monomer units close to the LCST was estimated to be approximately 5.2–5.8 mol%. The basicity of the copolymers decreased to a smaller extent above the LCST due to a decrease in dielectric constant of the environment. This indicates that there is no phase separation until the number of charged groups on the polymer is reduced to a critical limit.

The effect of polymer concentration in the range from 0.025 to 20 wt% on the critical solution temperature of the new copolymers was also studied. The results are shown in Figure 4. Interestingly, the critical solution temperature of the copolymers decreases with increase in polymer concentration and the effect is more pronounced in the more dilute regime.

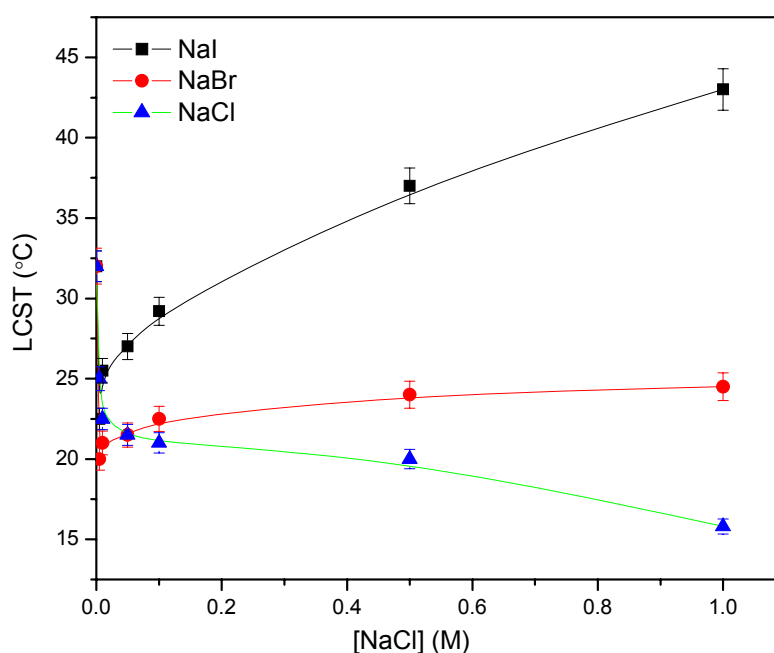
Figure 4. Effect of polymer concentration on the LCST in water.



3.4. Effect of Simple Salts and Cationic Surfactants on the LCST

The sensitivity of LCST to ionic species is of practical and theoretical importance. The effect of simple salts such as NaCl, NaBr, and NaI on the LCST of copolymers was studied, and the results for copolymer BCP1 is shown in Figure 5. The salts of chloride and bromide exerts a salting-out effect whereas iodide produces a salting-in effect. In general, inorganic ions disrupt hydrogen bonds and break the ordered structure of water which leads to hydrophobic interactions between the polymer chains. The extent to which the salting-out or salting-in effect occurs depends greatly on the charge and size of the ions. The observed trend in the LCST change may be related to a parameter called the viscosity B coefficient which is a measure of ion-water interactions. The coefficient values (mol^{-1}) for chloride, bromide and iodine ions are -0.007 , -0.042 , and -0.069 respectively. The values suggest that water structure-making effect by the ion increases with decrease in radius of the ion which causes the observed change in LCST of the copolymers [16]. Furthermore, other factors such as ion-dipole interactions, charge and size of the ions, also play a role in the salting-out or salting-in effects.

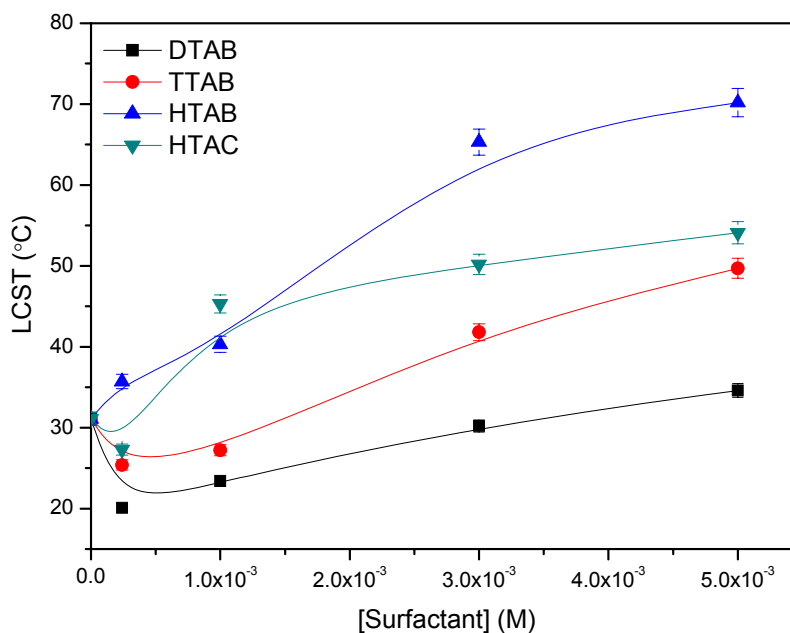
Figure 5. Effect of simple salts on the LCST of copolymer BCP-1.



The study of aqueous solutions of polymers and surfactants provides valuable insight into polymer-surfactant interactions and polymer-mediated surfactant micelle formation. The changes in LCST caused by the addition of a surfactant to a polymer solution are an indication of the strength and nature of interactions. The effect of cationic surfactants, dodecyl trimethylammonium bromide (DTAB), tetradecyl ammonium bromide (TTAB), hexadecyl trimethylammonium chloride (HTAC) on the LCST of BCP-1 is shown in Figure 6. Long chain surfactant molecules are known to form polymer-surfactant complexes through hydrophobic interactions between the alkyl tail of the surfactant and the polymer backbone. In very dilute solutions, the cationic surfactants behaved like simple electrolytes and exerted a salting-out effect on the polymer leading to an initial drop in LCST. Above the critical aggregation concentration (cac), which is generally about 1–3 orders of magnitude lower

than the critical micelle concentration (cmc) polymer-surfactant complexes are formed. The charged head groups of the surfactant molecules binding to the polymers give rise to electrostatic repulsion which stabilizes the polymer chain and causes the LCST to increase. The minima for the three surfactants in the LCST-surfactant concentration (Figure 6) relationship signify the onset of surfactant-polymer binding. No minimum was observed for the surfactant HTAB as the cac is expected to be very low because of its low cmc of $8 \times 10^{-4} \text{ mol}\cdot\text{dm}^{-3}$.

Figure 6. Effect of cationic surfactants on the LCST of copolymer BCP-1.



3.5. Microcalorimetric Study

The thermodynamic parameters of the polymer BCP-1 and BCP-4 during phase separation in water was studied using differential microcalorimetry and the data is shown in Table 2. By combining the data on the calorimetric enthalpy of transition ΔH with the LCST one can obtain insight on the enthalpy-entropy balance during phase transition. The enthalpy of phase transition of BCP1 and BCP4 were 24.35 and 24.41 $\text{J}\cdot\text{g}^{-1}$ respectively. These values correspond to about $4 \text{ kJ}\cdot\text{mol}^{-1}$ of repeating unit of the polymer, which reflect the energy required to break one hydrogen bond per monomer repeat unit. The value is comparable to those reported for amine based polymers of PNIPAM ($4.60 \text{ kJ}\cdot\text{mol}^{-1}$), and *N,N*-diethyl acrylamide ($2.94 \text{ kJ}\cdot\text{mol}^{-1}$). The variation in values observed is attributed to the nature of the amide group as well as on the experimental [16].

Table 2. Thermodynamic properties of copolymers measured using microcalorimetry.

Copolymer	LCST ^{Water} (°C)	ΔH ($\text{J}\cdot\text{g}^{-1}$)	C_p ($\text{J}\cdot\text{g}^{-1}\cdot\text{K}^{-1}$)	T_m (°C)
BCP-1	33.3	24.35	2.89	32.10
BCP-4	61.2	24.40	3.08	28.02

3.6. Viscosity Measurements

The solution properties of the polymers BCP-1 and BCP-4 were studied in dimethyl formamide (DMF) at 30, 40 and 50 °C. The intrinsic viscosity $[\eta]$ was calculated using the Huggins' equation as,

$$\frac{\eta_{sp}}{C_p} = [\eta] + k_H [\eta]^2 C_p \quad (7)$$

where η_{sp}/C_p , and K_H are the reduced viscosity and Huggins' constant respectively. The intrinsic viscosity data are shown in Figure 7. In general, the intrinsic viscosity of the polymers decreases with increase in temperature (negative slope). This clearly indicates that the polymer coils do not swell to a great extent in DMF, which is attributed to a decrease in thermodynamic interaction between the polymer and solvent with increase in temperature. Similar behavior has been reported for copolymers of acrylonitrile and MMA also in DMF. The equivalent hydrodynamic volume V_e of the polymers was calculated using the relative viscosity data by the method described by Narang and Garg [17]. This hydrodynamic volume is a measure of the size of a solvated polymer molecule at infinite dilution. The results summarized in Figure 8 show a decrease in V_e with increase in temperature further indicating a decrease in solvation of the polymer at high temperatures. The shape factor (ν) of the polymer chains was calculated as,

$$\nu = \frac{[\eta]}{V_e} \quad (8)$$

where $[\eta]$ and V_e are the intrinsic viscosity and equivalent hydrodynamic volume respectively. The value of ν for both the polymers at the three different temperatures studied was 3.0. This indicates that in the concentration range studied, the polymer chains are approximately spherical in shape.

Figure 7. Effect of temperature on the intrinsic viscosity of copolymers BCP-1 and BCP-4 in water.

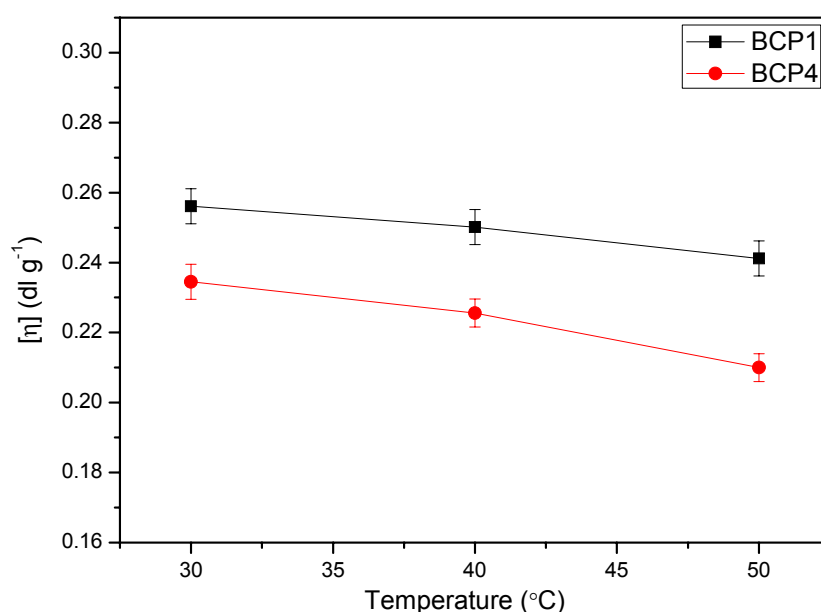
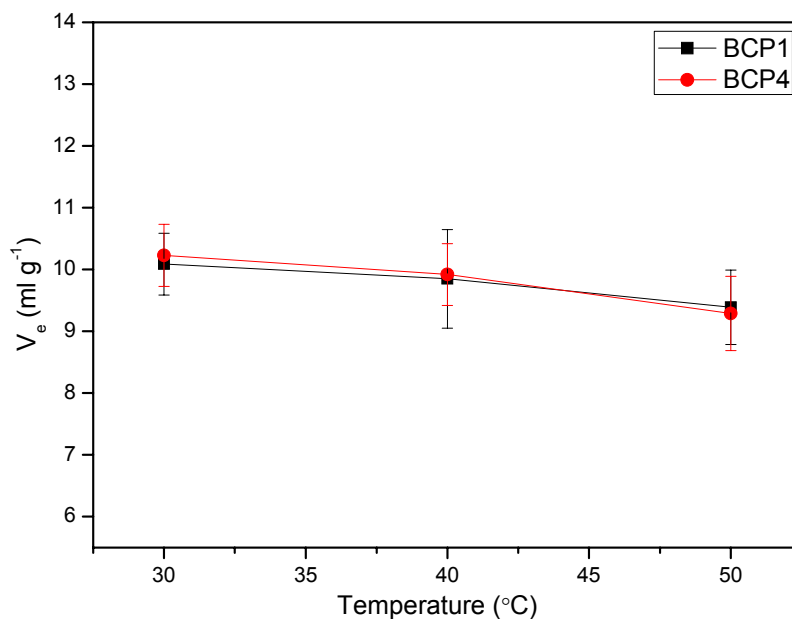
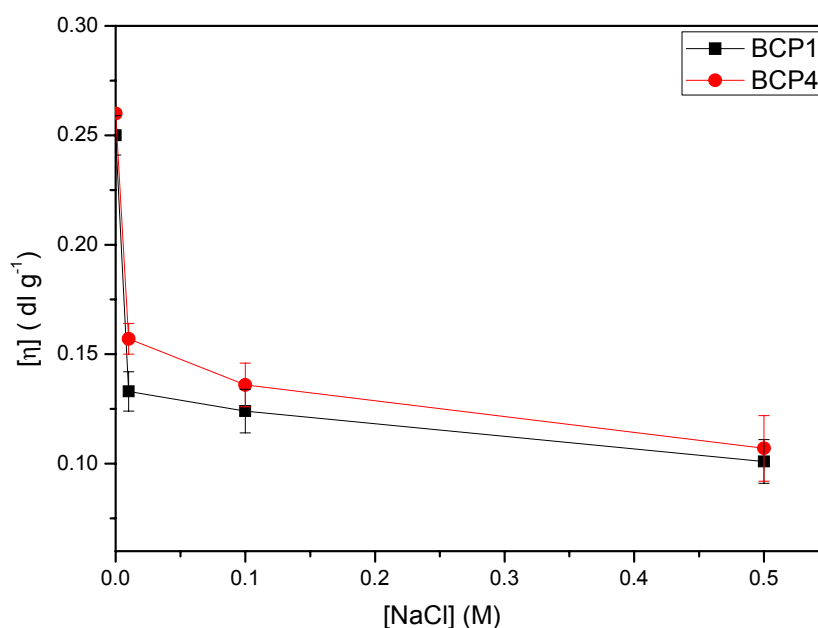


Figure 8. Effect of temperature on the equivalent hydrodynamic volume of copolymers BCP-1 and BCP-4 in DMF.



The intrinsic viscosity of the polymers BCP-1 and BCP-4 in solutions of various NaCl concentrations is shown in Figure 9. This study was performed to illustrate the effect of simple electrolytes on the viscosity of polymers and also to demonstrate the polyelectrolyte nature of these polymers of the class poly(amido-amines). With increase in NaCl concentration, the viscosity of the polymers decreases due to reduction in their coil size, this is similar to the behavior of polyelectrolytes and hydrophobically modified polyacrylates in solution.

Figure 9. Effect of NaCl concentration on the intrinsic viscosity of copolymers BCP-1 and BCP-4 measured at 25 °C.



3.7. Light Scattering Measurements

The molecular and thermodynamic parameters of the copolymers were determined by light scattering method and the results are summarized in Table 3. The A_2 values are positive which indicates good polymer-solvent interactions.

Table 3. Molecular and thermodynamic parameters of copolymers determined by light scattering technique in THF at 23 °C.

Copolymer	M_w (10^{-5} g·mol $^{-1}$)	R_h (nm)	A_2 (10^{-4} mol·cm 3 ·g $^{-2}$)
BCP-1	0.92	20.28	1.79
BCP-2	0.96	20.86	1.88
BCP-3	0.87	21.32	1.93
BCP-4	0.98	22.01	1.98

3.8. Glass Transition Temperature

The glass transition temperature (T_g) of the copolymers was determined from the mid-point of inflections of the DSC thermograms, and the values are shown in Table 4. The T_g of the copolymers is in-between that of their corresponding homopolymers, viz. PAcrNEP and PMMA. The copolymers showed only one T_g which indicates a high degree of mixing of the two monomers which is consistent with their statistical random distribution in the copolymer.

Table 4. Glass transition temperature of the copolymers.

Copolymer	T_g (°C)
BCP-1	114.12
BCP-2	111.20
BCP-3	109.36
BCP-4	109.00
PAcrNEP	108.32
PMMA	114.70

4. Conclusions

This study presented a new series of piperazine-containing ‘smart’ copolymers. The copolymers were water-soluble above 44 mol% of AcrNEP content and displayed LCST phenomena. The LCST could be tuned and controlled by varying the composition of copolymers, solution pH, salts and cationic surfactants. These water-soluble copolymers could further be modified and applied as rheological thickeners, and ionomers for nanoparticle preparation. Thus molecular heterogeneity plays an important role in altering the properties of water-soluble “smart” polymeric systems.

Acknowledgements

Financial support under NIEAcRF RI 8/09 GRD from Nanyang Technological University, National Institute of Education is gratefully acknowledged.

References

1. Okano, T.; Bae, Y.H.; Jacobs, H.; Kim, S.W. Thermally on-off switching polymers for drug permeation and release. *J. Control. Release* **1990**, *11*, 255-265.
2. Okuzaki, H.; Osada, Y. Electro-driven polyelectrolyte gel with biomimetic motility. *Electrochim. Acta* **1995**, *40*, 2229-2232.
3. Hoffman, A.S. The origins and evolution of 'controlled' drug delivery systems. *J. Control. Release* **2008**, *132*, 153-156.
4. Freitas, R.F.S.; Cussler, E.L. Temperature sensitive gels as extraction solvents. *Chem. Eng. Sci.* **1987**, *42*, 97-103.
5. Miyata, T.; Uragami, T.; Nakamae, K. Biomolecule-sensitive hydrogels. *Adv. Drug Delivery Rev.* **2002**, *54*, 79-98.
6. Schild, H.G. Poly(N-isopropylacrylamide): Experiment, theory and application. *Prog. Polym. Sci.* **1992**, *17*, 163-249.
7. Vaidya, A.A.; Lele, B.S.; Kulkarni, M.G.; Mashelkar, R.A. Thermoprecipitation and lysozyme from egg white using copolymers of N-isopropylacrylamide and acidic monomers. *J. Biotechnol.* **2001**, *87*, 95-107.
8. Alli, A.; Hazer, B. Poly(N-isopropylacrylamide) thermoresponsive cross-linked conjugates containing polymeric soyabean oil and/or polypropylene glycol. *Eur. Polym. J.* **2008**, *44*, 1701-1713.
9. Zhang, C.; Easteal, A.J. Study of free-radical copolymerization of N-isopropylacrylamide with 2-acrylamido-2-methyl-1-propanesulphonic acid. *J. Appl. Polym. Sci.* **2003**, *88*, 2563-2569.
10. Gürdağ, G.; Kurtuluş, B. Synthesis and characterization of novel poly(N-isopropylacrylamide-co-N,N'-dimethylaminoethyl methacrylate sulphate) hydrogels. *Ind. Eng. Chem. Res.* **2010**, *49*, 12675-12684.
11. González, N.; Elvira, C.; San Román, J. Novel dual-stimuli-responsive polymers derived from ethylpyrrolidine. *Macromolecules* **2005**, *38*, 9298-9303.
12. Mujumdar, S.K.; Siegel, R.A. Introduction of pH-sensitivity into mechanically strong nanoclay composite hydrogels based on N-isopropylacrylamide. *J. Polym. Sci. Part A: Polym. Chem.* **2008**, *46*, 6630-6640.
13. Yuk, S.H.; Cho, S.H.; Lee, S.H. pH/temperature-responsive polymer composed of poly(N,N-dimethylamino ethyl methacrylate-co-ethylacrylamide). *Macromolecules* **1997**, *30*, 6856-6859.
14. Uzgören, A.; Rzaev, Z.M.O.; Okay, G. Bioengineering functional copolymers: Synthesis and characterization of poly(N-isopropylacrylamide-co-3,4-2H-dihydropyran)s. *J. Polym. Res.* **2007**, *14*, 329-338.
15. Roshan Deen, G.; Gan, L.H. Determination of reactivity ratios and swelling characteristics of 'stimuli' responsive copolymers of N-acryloyl-N'-ethyl piperazine and methyl methacrylate. *Polymer* **2006**, *47*, 5025-5034.
16. Roshan Deen, G. Studies of Piperazine-Based Polymers and Hydrogels. Ph.D. dissertation, Nanyang Technological University, Singapore, 2000.

17. Asaduzamman, A.K.M.; Rakshit, A.K.; Devi, S. Solution properties of methyl methacrylate and acrylonitrile. *J. Appl. Polym. Sci.* **1993**, *47*, 1813-1819.

© 2012 by the authors; licensee MDPI, Basel, Switzerland. This article is an open access article distributed under the terms and conditions of the Creative Commons Attribution license (<http://creativecommons.org/licenses/by/3.0/>).